The Journal of Immunology

RESEARCH ARTICLE | AUGUST 30 2024

IFN Receptor 2 Regulates TNF-α–Mediated Damaging Inflammation during *Aspergillus* Pulmonary Infection

Agnieszka Rynda-Apple; ... et. al

J Immunol (2024) 213 (8): 1202–1211.
https://doi.org/10.4049/jimmunol.2200686

IFN Receptor 2 Regulates TNF-α–Mediated Damaging Inflammation during *Aspergillus* Pulmonary Infection

Agnieszka Rynda-Apple,* Jazmin Reyes Servin,† Julianna Lenz,† Julia Roemer,* Evelyn E. Benson,* Monica N. Hall,* and Kelly M. Shepardson*,†

The increased incidence of invasive pulmonary aspergillosis, caused by *Aspergillus fumigatus*, occurring in patients infected with severe influenza or SARS-CoV-2, suggests that antiviral immune responses create an environment permissive to fungal infection. Our recent evidence suggests that absence of the type I IFN receptor 2 subunit (IFNAR2) of the heterodimeric IFNAR1/2 receptor is allowing for this permissive immune environment of the lung through regulation of damage responses. Because damage is associated with poor outcome to invasive pulmonary aspergillosis, this suggested that IFNAR2 may be involved in *A. fumigatus* susceptibility. In this study, we determined that absence of IFNAR2 resulted in increased inflammation, morbidity, and damage in the lungs in response to *A. fumigatus* challenge, whereas absence of IFNAR1 did not. Although the *Ifnar2*$^{-/-}$ mice had increased morbidity, we found that the *Ifnar2*$^{-/-}$ mice cleared more conidia compared with both wild-type and *Ifnar1*$^{-/-}$ mice. However, this early clearance did not prevent invasive disease from developing in the *Ifnar2*$^{-/-}$ mice as infection progressed. Importantly, by altering the inflamed environment of the *Ifnar2*$^{-/-}$ mice early during *A. fumigatus* infection, by neutralizing TNF-α, we were able to reduce the morbidity and fungal clearance in these mice back to wild-type levels. Together, our results establish a distinct role for IFNAR2 in regulating host damage responses to *A. fumigatus* and contributing to an *A. fumigatus*–permissive environment through regulation of inflammation. Specifically, our data reveal a role for IFNAR2 in regulating TNF-α–mediated damage and morbidity during *A. fumigatus* infection. *The Journal of Immunology*, 2024, 213: 1202–1211.

The increase in the use of immunosuppressive therapies to treat human diseases over the past three decades has led to an increase in the number of invasive pulmonary fungal infections occurring (1–3). These invasive infections are most commonly caused by the filamentous fungus *Aspergillus fumigatus*, which has a global incidence of >300,000 cases/year. With the difficulty in diagnosis and a limited antifungal drug repertoire that often result in substantial toxicity, the mortality from invasive fungal infections remains very high (40–80%) (2, 4). In addition, toxicity-associated mortality is a common side effect of many of the available treatments (5). Additional complexity in treating aspergillosis, and an important contributor to pathological outcome to these invasive infections, is the high level of tissue/organ damage that the host incurs (6, 7). This damage can be inflicted by the pathogen, when a weak host response fails to limit fungal growth, and/or by the host, when a strong inflammatory response induced against the pathogen impairs the lung's vital function of gas exchange. Thus, there has been an increasing effort to redesign antifungal therapies in a way that augments host antifungal immune responses while minimizing host tissue injury caused by damaging inflammation. However, for these efforts to be successful, the specific immune mechanisms that protect the host from infection and/or subsequent tissue pathologies during aspergillosis must be identified.

Although it is well established that a compromised or malfunctioning immune system is required for opportunistic pathogens such as *A. fumigatus* to cause disease, concepts of what encompasses immunocompromised is continually being revised. *A. fumigatus* infection is known to occur in patients suffering from cystic fibrosis, tuberculosis, and drug-induced immunosuppression but also chronic obstructive pulmonary disease, sarcoidosis and influenza, suggesting that altered, either hypoactive or hyperactive, immune environments in the lung can be risk factors for development of *Aspergillus* lung disease (6, 8, 9). In particular, the recent increase in incidence of aspergillosis occurring in patients infected with either influenza or SARS-CoV-2, coupled with increased morbidity and mortality of these patients with *Aspergillus*-complicated influenza (10–14), suggests that antiviral immune responses result in a transiently suppressed lung immune environment that becomes permissive to fungal infection.

We, among others, have established that type I IFN signaling induced by influenza virus infection increases host susceptibility to

*Department of Microbiology and Cell Biology, Montana State University, Bozeman, MT; and †Department of Molecular and Cell Biology, University of California, Merced, Merced, CA

ORCIDs: 0009-0003-7738-3580 (J.R.S.); 0009-0009-7587-702X (J.L.); 0000-0001-9675-7945 (J.R.); 0000-0002-4009-4617 (M.N.H.); 0000-0003-3631-2594 (K.M.S.).

Received for publication September 14, 2022. Accepted for publication August 9, 2024.

This work was supported by the Division of Microbiology and Infectious Diseases, National Institute of Allergy and Infectious Diseases, National Institutes of Health (Grants R01AI04905 and K22AI153671); IDeA Networks of Biomedical Research Excellence at National Institute of General Medical Sciences, National Institutes of Health (Grant P20GM103474); Francis Family Foundation Parker B. Francis Fellowship; American Association of Immunologists Careers in Immunology Fellowship; MSU Agriculture Experiment Station; and M.J. Murdock Charitable Trust.

K.M.S. designed and performed experiments, analyzed data, and contributed to writing of the paper. J.R., J.R.S., and J.L. performed experiments and analyzed data. E.E.B. and M.N.H. performed experiments. A.R.-A. designed experiments, analyzed data, and contributed to writing of the paper.

The content of this publication is solely the responsibility of the authors and does not necessarily represent the official views of the National Institutes of Health.

Address correspondence and reprint requests to Dr. Kelly M. Shepardson, University of California, Merced, 5200 North Lake Road, Merced, CA 95343. E-mail address: kshepardson2@ucmerced.edu

The online version of this article contains supplemental material.

Abbreviations used in this article: ALI, acute lung injury; Ang, angiopoietin; BALF, bronchoalveolar lavage fluid; CGD, chronic granulomatous disease; GMS, Gomori's methenamine silver; IAV, influenza A virus; IFNAR1, IFN receptor 1 subunit; IFNAR2, IFN receptor 2 subunit; i.n., intranasal; IPA, invasive pulmonary aspergillosis; i.t., intratracheal; LDH, lactate dehydrogenase; LH, lung homogenate; MDC, minimum detectable concentration; MSU, Montana State University; mTNF-α, mouse TNF-α; p.i., postinfection; SigF, Siglec-F; WT, wild-type.

https://doi.org/10.4049/jimmunol.2200686

secondary bacterial infections (15–19). However, the evaluation of the effect that type I IFN signaling may have on disease severity had primarily been considered in IFN receptor 1 subunit (IFNAR1)-deficient mice, where IFN receptor 2 subunit (IFNAR2) is still present. Our recent evidence generated using *Ifnar2*$^{-/-}$ mice revealed that absence of either IFNAR1 or IFNAR2 results in very distinct disease phenotypes in response to influenza virus infection (20). Specifically, we found that absence of IFNAR2 led to exacerbated influenza disease that correlated with an increase in damage biomarkers. Because one of the main factors involved in the pathological outcome of invasive pulmonary aspergillosis (IPA) is the level of host tissue damage, this prompted us to investigate whether and how the absence of either IFNAR subunit contributes to the resolution of *A. fumigatus* infection. In this article, we report that IFNAR2 is involved in regulating the damage response during pulmonary *A. fumigatus* infection, and that absence of IFNAR2 contributes to an *A. fumigatus*–permissive environment through dysregulation of inflammation. Importantly, these results expand the role of IFNAR signaling to include contributions from both subunits and highlight the need to understand how the individual IFNAR subunits contribute to infection outcome.

Materials and Methods

Mice

Male and female wild-type (WT) C57BL/6 (Jackson Laboratories), *Ifnar1*$^{-/-}$ (originally designed and bred at Montana State University [MSU]) (21), and *Ifnar2*$^{-/-}$ [Ifnar2tm1(KOMP)Vlcg, originally purchased from UC Davis Knockout Mouse Project (KOMP) Repository] mice were bred and maintained at both MSU (Bozeman, MT) Animal Resources Center and University of California, Merced (Merced, CA) under pathogen-free conditions. All mice used in this study were between 7 and 12 wk of age at the initiation of experiment. Mice were weighed and monitored for signs of morbidity and mortality. All care and procedures were in accordance with the recommendations of the National Institutes of Health, the United States Department of Agriculture, and the *Guide for the Care and Use of Laboratory Animals*, 8th ed. (22). Animal protocols were reviewed and approved by both the MSU and UCM Institutional Animal Care and Use Committee. MSU and University of California, Merced (UCM) are accredited by the Association for Assessment and Accreditation of Laboratory Animal Care (no. 713 and 001318).

Fungal cultures and growth conditions

A. fumigatus strain CEA10 (CBS144.89) (a kind gift from R.A. Cramer at Geisel School of Medicine at Dartmouth College) was used in all experiments. All strains were grown on glucose minimal medium with 1.5% agar at 37°C for 5 d. Conidia were dislodged from plates with a cell scrapper, resuspended in 0.01% Tween 20, and filtered through sterile 48-μm nylon mesh screen (Sefar America). Conidia were counted using a hemacytometer, washed once with PBS, and resuspended in PBS at a final concentration of $6–8 \times 10^8$ conidia/ml.

Inoculations and challenge

Nonsurgical intratracheal (i.t.) inoculations were performed as described previously for all inoculations and challenges (15, 20, 23). In brief, a blunt 20G needle attached to a 1-ml syringe was advanced into the trachea to instill the indicated number of conidia or PFUs. For fungal inoculation, mice were inoculated within a range of $6–8 \times 10^7$ *A. fumigatus* conidia (24), and similar results and trends (fold changes) were found to occur within this range of doses. For virus inoculation, mice were inoculated with 100 μl of PBS or 0.1 LD_{50} (1500 PFUs) of influenza A virus (IAV) strain A/PR8/8/34 (PR8; H1N1).

Histological analysis

A. fumigatus–challenged mice were euthanized at indicated times. For histological studies, the lungs were inflated with 10% buffered formalin, fixed, and embedded in paraffin to generate 5-μm sections stained with H&E or Gomori's methenamine silver (GMS) stain for microscopy. Contiguous tissue sections were imaged using a Nikon Eclipse 80i microscope and NIS elements BR imaging system and software (Nikon, Melville, NY) or an EVOS M7000 Imaging System (ThermoFisher Scientific) at 2×, 4×, 20×, and 40× objective magnification. Experimental conditions/groups were blinded for image capture.

Fungal burden/germination analysis

For experiments looking at CFUs, mice were sacrificed 24 h postinfection (p.i.). Whole lung homogenate (LH) samples were serially diluted and plated onto glucose minimal media plates and incubated at 37°C, and CFUs were counted between 18 and 24 h after plating. To assess relative fungal burden in lungs, we sacrificed mice at 48 h postinoculation. Lungs were harvested and snap frozen using a BioSqueezer (Biospec Products, Bartlesville, OK) and liquid nitrogen. Samples were freeze dried, homogenized with glass beads on a Mini-Beadbeater (BioSpec Products, Bartlesville, OK), and DNA extracted with the E.N.Z.A. fungal DNA kit (Omega Bio-Tek, Norcross, GA). Quantitative PCR was performed as described previously (25). In brief, all DNA quantity and quality were assessed with a NanoDrop 1000 spectrophotometer (NanoDrop Technologies, Wilmington, DE). Working dilutions of 100 ng/μl were made for use in PCR mixtures, which each contained 500 ng of total DNA. A modified TaqMan probe/primer set (modified probe, 56-FAM [FAM]/AGCCAGCGGCCCGCAAATG/3IABLFQ [Iowa black fluorescein quencher; Integrated DNA Technologies]) amplified the 18S region of *A. fumigatus*. Six-point standard curves were calculated using serial dilutions of CEA10 genomic DNA. Total fungal DNA was calculated from the threshold cycle value from the appropriate standard curve and normalized to input DNA concentration. Each sample was amplified in triplicate. To assess fungal germination, as previously described (26), we quantified the percent germination of *A. fumigatus* by manually counting ~50–100 fungal conidia and germlings at ×20 or ×40 magnification on the histological GMS slides by using a standard upright microscope.

Preparation of bronchoalveolar lavage fluid samples, cytokine analyses, and flow cytometry

Mice were euthanized by i.p. administration of 90 mg/kg sodium pentobarbital. Bronchoalveolar lavage (BAL) was performed by washing the lungs with 2 ml of PBS + 3 mM EDTA (20), and cellular composition was determined by hemocytometer cell counts and differential counts of cytospins after staining with Quick-Diff solution (Siemens; Medical Solutions Diagnostics, Tarrytown, NY). Cell-free bronchoalveolar lavage fluid (BALF) was used to determine levels of soluble receptor for advanced glycation end products (31.3–2000 pg/ml) and angiopoietin (Ang) 2 (Ang2; 39.1–2500 pg/ml) (R&D Systems, Minneapolis, MN) and Ang1 (31.25–2000 pg/ml; Novus Biologicals) using ELISA kits. Results from analysis of BALF samples are reported as means ± SD from four or more mice per group. Cell-free BALF was also used to determine levels of TNF-α (minimum detectable concentration [MDC]; 1.9 pg/ml), IL-6 (MDC; 0.9 pg/ml), CCL2 (MCP1, MDC; 1.2 pg/ml), MIP-1a (MDC; 1.0 pg/ml), and KC (CXCL1, MDC; 1.54 pg/ml) using the LEGENDplex bead array assay kits (BioLegend, San Diego, CA). LEGENDplex beads were acquired on LSRII running FACSDiva software (both obtained from BD Bioscience). To harvest the single-cell suspension from mouse lungs (referred to as LH in Fig. 3), we followed previously reported methods (27), where the whole lungs were minced and digested in buffer containing 2.2 mg/ml collagenase type IV (Worthington), 1 U/ml DNase 1 (ThermoScientific), and 5% FBS at 37°C for 45 min. The digested samples were passed through an 18-gauge needle, incubated in RBC lysis buffer (Life Technologies), neutralized in PBS, passed through 100-μm pore filter, and counted. The Abs used for the flow cytometry analysis of different populations included CD45 (BV510 or allophycocyanin-Cyanine7; BioLegend), Ly6G (FITC; BioLegend), Siglec-F (SigF; PE; BioLegend), IA/IE (MHC-II) (BV510 or allophycocyanin; BioLegend), CD64 (BV421; BioLegend), CD11b (PerCP/Cyanine5.5; BioLegend), and DAPI just before running. The gating strategies for each of the cell populations are indicated in Supplemental Fig. 4. The data were collected from an LSRII running FACSDiva software (both obtained from BD Biosciences) and analyzed with FlowJo version 10.9.0.

Morbidity, mortality, lactate dehydrogenase, and albumin

Mice (male and female) were weighed daily and assessed for signs of morbidity and mortality. Morbidity/Mortality was measured as percent weight loss from day 0 (day of infection) until all mice either regained their initial weight or reached a defined clinical end point (>20% body weight loss). Lactate dehydrogenase (LDH) in the cell-free BALF was measured using the CytoTox 96 Non-Radioactive Cytotoxicity Assay (Promega), and albumin in the cell-free BALF was measured using QuantiChrom BCG Albumin Assay Kit (BioAssay Systems) following the manufacturer's protocols.

TNF-α neutralization and recombinant mouse TNF-α treatment

Mice received the indicated doses of recombinant mouse TNF-α (mTNF-α; 1 μg/dose; BioLegend) by intranasal (i.n.) instillation. We treated the mice with 1 μg of mTNF-α at both 6 and 30 h after *A. fumigatus* infection and did these treatments i.n. instead of i.t. to reduce the amount of liquid entering the lung and any damage associated with that. Thus, we used 1 μg of mTNF-α at each of the two administrations over the course of the experiment (6 and 30 h) to ensure there would be sufficient levels of TNF-α in the lung. Neutralization of TNF-α was performed using 0.5 mg of *InVivo*Mab anti–TNF-α (BioXCell; clone XT3.11), and as a control the manufacturer recommended *InVivo*MAb rat IgG1 isotype control (BioXCell; clone HRPN) administered i.p. 6 h after *A. fumigatus* infection.

Statistical analyses

All statistical analyses were performed with Prism 10.1.0 software (GraphPad Software, San Diego, CA). The log-rank test and Gehan-Breslow-Wilcoxon test were performed for statistical analysis of the survival curve. For animal experiments, nonparametric analyses (Kruskal-Wallis with Dunn's multiple comparisons and Mann–Whitney *U* test with single comparisons) and parametric analyses (one-way ANOVA test with Dunnett's multiple comparisons and paired *t* test) were performed. All error bars represent SDs, and significance is noted as follows: $^{NS}p > 0.05$, $*p \leq 0.05$, $**p \leq 0.01$, $***p \leq 0.001$, $****p \leq 0.0001$.

Results

Although *A. fumigatus* is known to cause disease in immunocompromised patients, an increasing number of reports point to IPA as an emerging post-IAV complication (10–14, 28–33). Consistent with the clinical data and recently published reports on influenza-associated IPA, we also found that WT mice challenged with *A. fumigatus* at day 7 post-IAV, which in both mice and humans marks increased host susceptibility to secondary infections (15–17), had higher lung fungal burden at 24 h after *A. fumigatus* infection when compared with *A. fumigatus*–only infected mice (Supplemental Fig. 1A). Importantly, we also found that the higher fungal burden in *A. fumigatus*–superinfected mice corresponded with increased LDH levels, a tissue damage biomarker, in the BALF (Supplemental Fig. 1B). This suggested that antiviral host responses could contribute to exacerbation of otherwise benign *A. fumigatus* infection through increased pulmonary damage.

Our previous data suggest that the IFNAR2 subunit of the type I IFN receptor plays a role in regulating damage during pulmonary infection (15, 20). Therefore, we sought to determine whether IFNAR2 also has a role in contributing to establishment of a lung environment permissive to *A. fumigatus* infection. Interestingly, we found that *Ifnar2*$^{-/-}$ mice cleared more conidia (decreased fungal CFUs/fungal burden) (Fig. 1A) early at 24 h after *A. fumigatus* compared with *Ifnar1*$^{-/-}$ and WT mice. Our data also correlated with previous reports showing higher fungal burden in *Ifnar1*$^{-/-}$ mice compared with WT mice at this time point (24, 34, 35). These results suggest that presence of IFNAR1 is both required and sufficient for early fungal clearance of conidia in vivo. Furthermore, that the WT mice were less efficient at clearing *A. fumigatus* compared with the *Ifnar2*$^{-/-}$ mice suggests that the presence of IFNAR2 may interfere with IFNAR1-mediated fungal clearance. Importantly, at this early time point the *Ifnar2*$^{-/-}$ mice showed increased weight loss when compared with *Ifnar1*$^{-/-}$ and WT mice (Fig. 1B), suggesting that the improvement in fungal clearance came at a cost of increased morbidity, likely because of inflammation and damage. Increased cellular infiltrate can be associated with increased weight loss and inflammation during infection; therefore, we next sought to determine whether there were differences in cell recruitment. We did not find any significant differences in the number of neutrophils or macrophages (based on differential counts) in the BALF collected from *Ifnar2*$^{-/-}$, *Ifnar1*$^{-/-}$, or WT mice at 24 h after *A. fumigatus* (Fig. 1C).

To investigate the cause of the increased morbidity of the *A. fumigatus*–infected *Ifnar2*$^{-/-}$ mice, we next examined whether there were differences in biomarkers associated with damage responses. Indeed, at 24 h after *A. fumigatus* infection, the lungs of

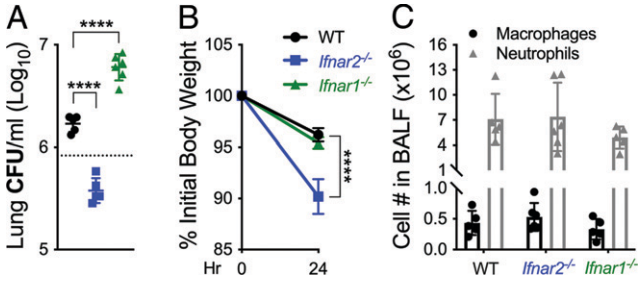

FIGURE 1. Mice deficient in IFNAR2 have increased fungal clearance and increased morbidity 24 h p.i. WT ($n = 5$), *Ifnar2*$^{-/-}$ ($n = 5$), and *Ifnar1*$^{-/-}$ ($n = 6$) mice were infected with 6×10^7 *A. fumigatus* conidia on day 0 (infection model shown). (**A**–**C**) CFUs from LH (A), weight loss as a percent of day 0 (initial body weight) (B), and differential counts on cells from the BALF (C) were analyzed 24 h p.i. Two independent experiments were performed, and data are shown as the representative results. One-way ANOVA test with Dunnett's multiple comparisons was performed for statistical analyses. All error bars represent SDs. $****p < 0.0001$.

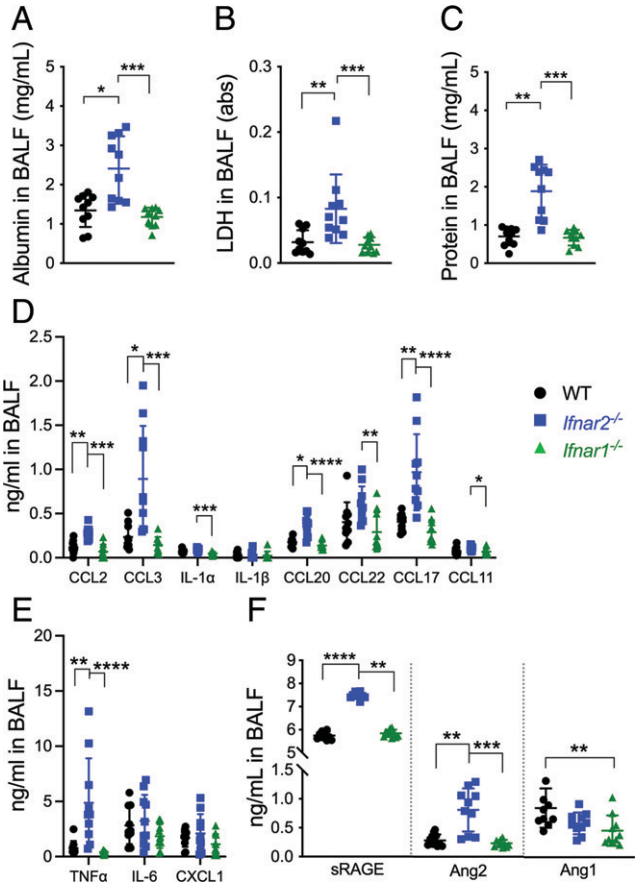

FIGURE 2. Increased level of biomarkers of damage/inflammation in the absence of IFNAR2 during *A. fumigatus* infection. WT, *Ifnar2*$^{-/-}$, and *Ifnar1*$^{-/-}$ mice were infected with 6×10^7 *A. fumigatus* conidia on day 0. (**A**–**F**) Albumin (A), LDH (B), protein (C), bead array cytokines/chemokines (D and E), and biomarker (F) level by ELISA were measured from cell-free BALF 24 h p.i. Two independent experiments were performed, and data are shown as the combined results (WT group, $n = 10$; *Ifnar2*$^{-/-}$ group, $n = 10$; *Ifnar1*$^{-/-}$ group, $n = 10$). The Kruskal-Wallis test with Dunn's multiple comparisons was performed for statistical analyses. All error bars represent SDs. $*p < 0.05$, $**p < 0.01$, $***p < 0.001$, $****p < 0.0001$.

Ifnar2$^{-/-}$ mice compared with *Ifnar1*$^{-/-}$ and WT mice had increased levels of albumin, LDH, and overall protein content (Fig. 2A–C). This suggests that IFNAR2 is important for regulating vascular leakage and cellular damage during *A. fumigatus* infection. Although *A. fumigatus* infection in *Ifnar2*$^{-/-}$ mice did not result in increased phagocyte recruitment (Fig. 1C), the levels of many inflammatory cytokines and chemokines were higher in these mice when compared with *Ifnar1*$^{-/-}$ and WT mice (Fig. 2D–E). We also found that markers of epithelial and endothelial damage, soluble receptor for advanced glycation end products (36) and Ang2 (37), but not Ang1 (Fig. 2F), were increased in the *Ifnar2*$^{-/-}$ mice compared with *Ifnar1*$^{-/-}$ and WT mice. These results suggest that IFNAR2 is involved in regulating not just the inflammatory environment but also lung integrity, specifically damage to the lung epithelium, early on during *A. fumigatus* infection. Because we found increased inflammatory markers in the *Ifnar2*$^{-/-}$ mice at 24 h after *A. fumigatus*, we analyzed the lung cellularity of both the BALF and the lung (LH) at this time point (Fig. 3, Supplemental Fig. 4). We found no difference in the number of total cells from both the BALF and the LH from *Ifnar2*$^{-/-}$, *Ifnar1*$^{-/-}$, or WT mice at 24 h after *A. fumigatus* (Fig. 3D, 3I). Further, we observed equivalent levels of neutrophils (Ly6G^{+} CD11b^{+}), monocytes (CD11b^{hi}CD64^{-}MHCII^{-}), interstitial macrophages (LH only; CD11b^{hi}CD64^{+}), and alveolar macrophages (Ly6G^{-}, CD11b^{+}, SigF^{+}) in both the BAL and the LH of *Ifnar2*$^{-/-}$, *Ifnar1*$^{-/-}$, or WT mice at 24 h after *A. fumigatus* (Fig. 3). These results show no difference in cellularity at this time point, similar to results found in an IAV–*A. fumigatus* model (27), suggesting other mechanisms, such as effector mechanisms, may be involved in the clearance and damage phenotypes.

Thus far, our results pointed to the presence of IFNAR2 as important in regulating damage responses up to 24 h after *A. fumigatus* infection. To understand the involvement of lung damage in *A. fumigatus* infection outcome, we then sought to determine the damage response over the course of infection, from initial recognition (~6 h) to when invasive growth of this fungus begins to occur (~48 h). We found that when compared with WT and *Ifnar1*$^{-/-}$ mice, the damage response in the *Ifnar2*$^{-/-}$ mice, as measured by albumin levels, was already increased by 6 h after *A. fumigatus* challenge and remained elevated at 24 h p.i., maintaining this nonstatistically significant elevated level at 48 h p.i. (Figs. 2A, 4A, 4B). Because *A. fumigatus* growth favors a more damaged environment, we next sought to determine how the various degrees of early damage affected infection progression in WT, *Ifnar1*$^{-/-}$, and *Ifnar2*$^{-/-}$ mice. Although at 24 h p.i. there was initial control of fungal clearance in the *Ifnar2*$^{-/-}$ mice (Fig. 1A), we found that this did not prevent invasive growth from occurring by 48 h p.i. (Fig. 4C). As such, at 48 h p.i., lungs of *Ifnar2*$^{-/-}$ mice had an increase in hyphal growth via increased germination (26, 38–40) when compared with *Ifnar1*$^{-/-}$ and WT mice (Fig. 4E). This increased germination could also be a result of the increased albumin levels in the lungs of the *Ifnar2*$^{-/-}$ mice because albumin supplementation has been shown to increase *A. fumigatus* germination (41). Histological examination also revealed large areas of inflammation (infiltrates, edema) surrounding the fungal growth in the *Ifnar2*$^{-/-}$ mice (Fig. 4C), suggesting that the increased damage was involved in allowing for invasive growth. We then measured the fungal burden at 48 h p.i. to determine whether the damage was allowing for progression of *A. fumigatus* infection. We found that the *Ifnar2*$^{-/-}$ mice had similar levels of lung fungal burden as WT mice and *Ifnar1*$^{-/-}$ mice at 48 h p.i. (Fig. 4D). These results suggest that early damage, although associated with more efficient clearance of conidia, may be contributing to a favorable environment for fungal growth to occur. Consistent with the increased hyphal growth and inflammation in the lungs of the *Ifnar2*$^{-/-}$ mice at 48 h after *A. fumigatus* infection, we also found that these mice continued to experience significant weight loss compared with *Ifnar1*$^{-/-}$ and WT mice (Fig. 4F), suggesting further increases in the morbidity of the *Ifnar2*$^{-/-}$ mice. We next sought to determine whether the morbidity affected survival to *A. fumigatus*. Interestingly, we found that *Ifnar2*$^{-/-}$, *Ifnar1*$^{-/-}$, and WT mice all had a median survival time of 3 d p.i., with all *Ifnar1*$^{-/-}$ mice succumbing to *A. fumigatus*, similar to what has been previously found with *Ifnar1*$^{-/-}$ mice (24) (Fig. 5A). Although there was substantial mortality, the surviving mice recovered to their starting weight (Fig. 5B).

Despite early inflammation and initial containment of infection, *Ifnar2*$^{-/-}$ mice still developed invasive disease (hyphal growth) and lung tissue damage by 48 h after *A. fumigatus* infection. Thus, we sought to determine whether the early inflammatory response was

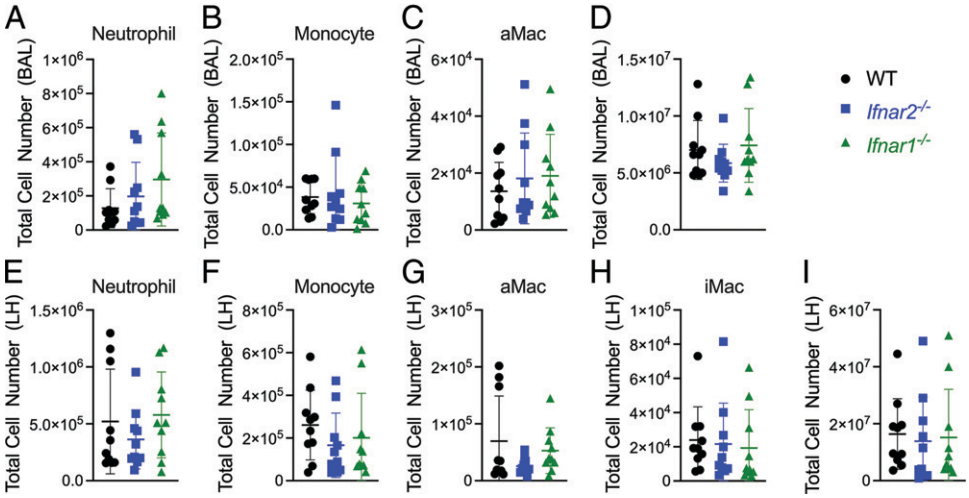

FIGURE 3. Absence of IFNAR2 or IFNAR1 does not affect lung cellularity during *A. fumigatus* infection. WT, *Ifnar2*$^{-/-}$, and *Ifnar1*$^{-/-}$ mice were infected with 6×10^7 *A. fumigatus* conidia on day 0. Mice were euthanized at 24 h p.i. with *A. fumigatus* for lung cellularity experiments on the BAL cells (**A–D**) and LH cells (**E–I**). All cell numbers were acquired by flow cytometry as indicated: (A and E) neutrophils (CD45^{+}Ly6G^{+}CD11b^{+}), (B and F) monocytes (CD45^{+}Ly6G^{-}SigF^{-}CD11b^{hi}CD64^{-}MHCII^{-}) (C and G) alveolar macrophages (aMacs) (CD45^{+}Ly6G^{-}SigF^{+}CD11b^{+}), (D and I) total lung cells, and (H) interstitial macrophages (iMac) (CD45^{+}Ly6G^{-}SigF^{-}CD11b^{hi}CD64^{+}). Two independent experiments were performed, and data are shown as the combined results (WT group, $n = 10$; *Ifnar2*$^{-/-}$ group, $n = 10$; *Ifnar1*$^{-/-}$ group, $n = 10$). The Kruskal-Wallis test with Dunn's multiple comparisons was performed for statistical analyses. All error bars represent SDs.

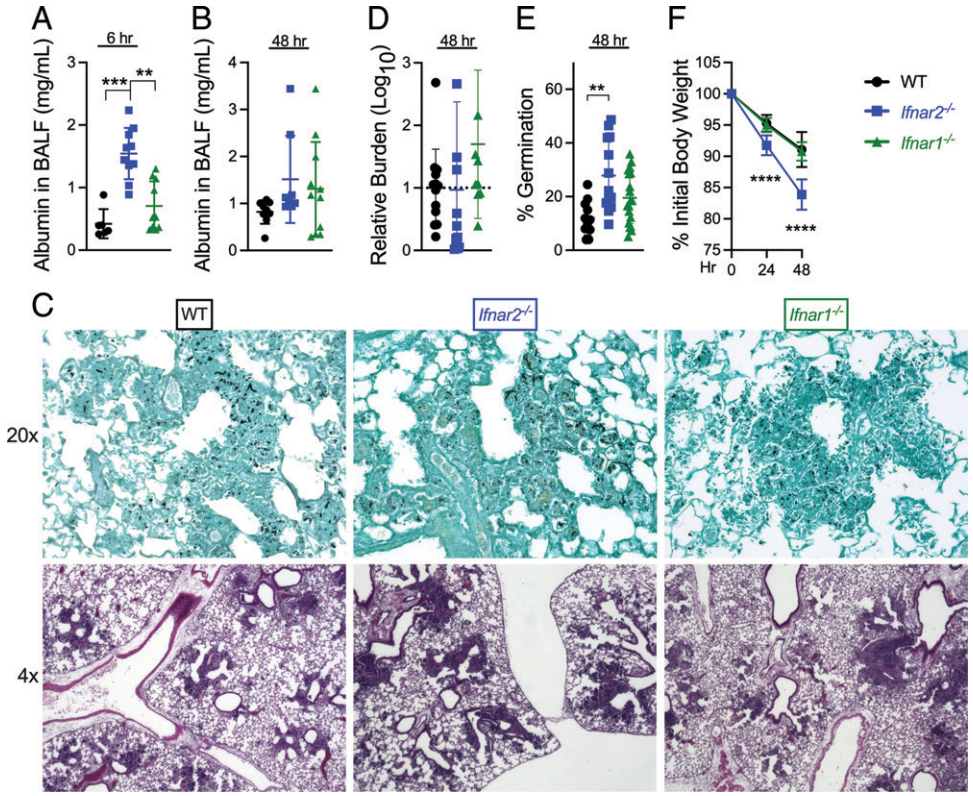

FIGURE 4. Early IFNAR2-regulated damage response may create an environment permissive to hyphal growth. WT, *Ifnar1*$^{-/-}$, and *Ifnar2*$^{-/-}$ mice were infected with 6–8 × 10^7 *A. fumigatus* conidia i.t. on day 0. (**A**) Albumin from cell-free BALF was measured at 6 h p.i. Two independent experiments were performed, and data are shown as the combined results (WT group, $n = 6$; *Ifnar2*$^{-/-}$ group, $n = 10$; *Ifnar1*$^{-/-}$ group, $n = 10$). (**B**) Albumin from cell-free BALF was measured at 48 h p.i. Three independent experiments were performed, and data are shown as the combined results (WT group, $n = 9$; *Ifnar2*$^{-/-}$ group, $n = 9$; *Ifnar1*$^{-/-}$ group, $n = 10$). (**C** and **E**) Representative images from GMS- (original magnification ×20) and H&E (original magnification ×4)-stained lung sections from 48 h p.i. (C) and percent germination at 48 h p.i. (E) (data are shown as the combined results from multiple images from one experiment). (**D**) Relative fungal burden measured by qPCR at 48 h p.i. (three experiments were performed, and data are shown as the combined results of the fold change compared with WT mice, not all groups were in each experiment; WT group, $n = 13$; *Ifnar2*$^{-/-}$ group, $n = 12$; *Ifnar1*$^{-/-}$ group, $n = 10$). (**F**) Weight loss as a percent of day 0 (initial body weight) was measured (two independent experiments were performed, and data are shown as the combined results, not all groups were in each experiment; WT group, $n = 15$; *Ifnar2*$^{-/-}$ group, $n = 17$; *Ifnar1*$^{-/-}$ group, $n = 11$). The Kruskal-Wallis test with Dunn's multiple comparisons was performed for statistical analyses. All error bars represent SDs. $^{**}p < 0.01$, $^{***}p < 0.001$, $^{****}p < 0.0001$.

responsible for this detrimental outcome. To begin to understand this, we neutralized TNF-α, the most abundant proinflammatory cytokine we found in the *Ifnar2*$^{-/-}$ mice at 24 h p.i. (Fig. 2E). Our results show that neutralizing TNF-α at 6 h after *A. fumigatus* resulted in decreased fungal clearance to the level of WT mice (both isotype and nontreated controls) (Fig. 6A). Importantly, neutralization of TNF-α also decreased the morbidity of the *Ifnar2*$^{-/-}$ mice, shown by decreased weight loss compared with isotype-treated *Ifnar2*$^{-/-}$ mice (Fig. 6B). We also found that neutralization of TNF-α in *Ifnar2*$^{-/-}$ mice reduced their damage response because the albumin level was decreased compared with the isotype-treated *Ifnar2*$^{-/-}$ and was similar to the isotype and nontreated WT levels (Fig. 6C). Interestingly, the decrease in morbidity of the anti–TNF-α–treated *Ifnar2*$^{-/-}$ mice was not associated with a significant decrease in neutrophil

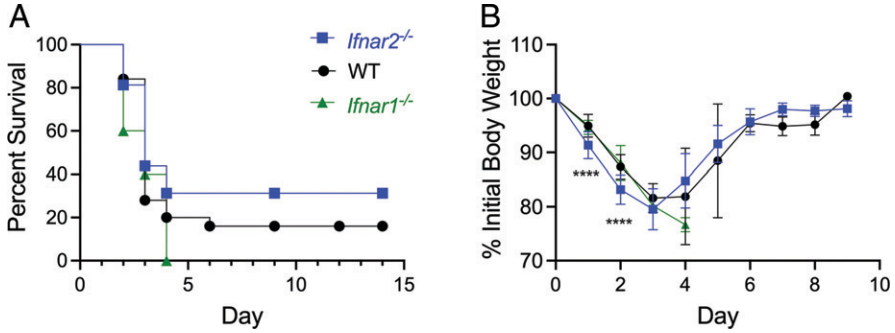

FIGURE 5. No difference in survival between *Ifnar2*$^{-/-}$ and WT mice. WT, *Ifnar1*$^{-/-}$, and *Ifnar2*$^{-/-}$ mice were infected with 6 × 10^7 *A. fumigatus* conidia i.t. on day 0. (**A** and **B**) Survival (A) and weight (B) were monitored daily. Three independent experiments were performed (WT group, $n = 18$; *Ifnar2*$^{-/-}$ group, $n = 16$), and one independent experiment was performed (WT group, $n = 7$; *Ifnar1*$^{-/-}$ group, $n = 5$), and data are shown as the combined results of all experiments. The log-rank test and Gehan-Breslow-Wilcoxon test were performed for statistical analysis of the survival curve, and the Kruskal-Wallis test with Dunn's multiple comparisons was performed for statistical analysis of day 1 and day 2 weights. Comparisons are WT group versus *Ifnar2*$^{-/-}$ group. $^{****}p < 0.0001$.

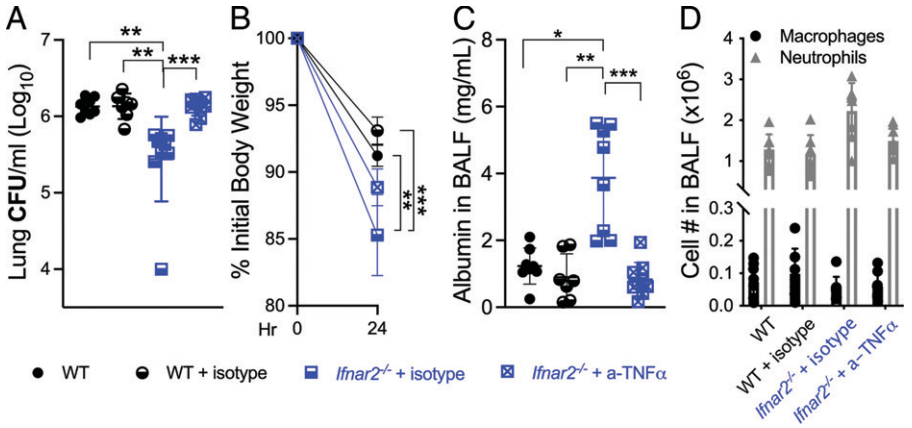

FIGURE 6. Role for TNF-α in damage and fungal clearance during *A. fumigatus* infection in WT and *Ifnar2*$^{-/-}$ mice. WT and *Ifnar2*$^{-/-}$ mice were infected with 8×10^7 *A. fumigatus* conidia i.t. on day 0 and were treated with anti–TNF-α or isotype Ab i.p. at 6 h p.i. (**A**–**D**) CFUs from LH (A), weight loss as a percent of day 0 (initial body weight) (B), and albumin were measured from cell-free BALF 24 h p.i. (C), and differential counts on cells from the BALF were analyzed 24 h p.i. (D). Two independent experiments were performed, and data are shown as the combined results (A/B: WT group, $n = 8$; WT + isotype group, $n = 7$; *Ifnar2*$^{-/-}$ + anti–TNF-α group, $n = 10$; *Ifnar2*$^{-/-}$ + isotype group, $n = 9$; C/D: WT group, $n = 8$; WT + isotype group, $n = 7$; *Ifnar2*$^{-/-}$ + anti–TNF-α group, $n = 9$; *Ifnar2*$^{-/-}$ + isotype group, $n = 8$). The Kruskal-Wallis test with Dunn's multiple comparisons (A and C) and the Mann–Whitney *U* test (B) were performed for statistical analyses. All error bars represent SDs. $^*p < 0.05$, $^{**}p < 0.01$, $^{***}p < 0.001$.

recruitment compared with isotype-treated *Ifnar2*$^{-/-}$ and WT mice (Fig. 6D), which is not what has been reported to occur with TNF-α blockage in WT mice (42). Further, we found that neutralization of TNF-α in WT mice did not significantly alter their response to fungal clearance, weight loss, or damage response compared with isotype-treated WT mice (Supplemental Fig. 2A-C), suggesting that high TNF-α levels are associated with the damage phenotype found during infection. This suggests there may be a differential role for TNF-α in the context of IFNAR signaling. To further address the role of TNF-α in regulation of *A. fumigatus* outcome, we next investigated whether treatment of the *Ifnar1*$^{-/-}$ mice with recombinant mTNF-α would lead to exacerbated progression of aspergillosis, mimicking what we found in the *Ifnar2*$^{-/-}$ mice. We found that treatment of the *Ifnar1*$^{-/-}$ mice with mTNF-α led to an increase in hyphal growth/germination compared with the PBS-treated *Ifnar1*$^{-/-}$ mice, but still less hyphal growth than PBS-treated WT mice (Fig. 7A, 7B) (26, 38–40). Treatment of the *Ifnar1*$^{-/-}$ mice with mTNF-α also led to a significant increase in weight loss compared with the PBS-treated WT mice and a nonstatistically significant increase compared with PBS-treated *Ifnar1*$^{-/-}$ mice (Fig. 7C). Further, we found that treatment of WT mice with mTNF-α after *A. fumigatus* infection resulted in similar weight loss and germination rates compared with WT mice that did not receive mTNF-α after *A. fumigatus* infection (Supplemental Fig. 3A–C). This indicates that this mTNF-α treatment was not sufficient to lead to altered responses of WT mice. Together, these results suggest that although

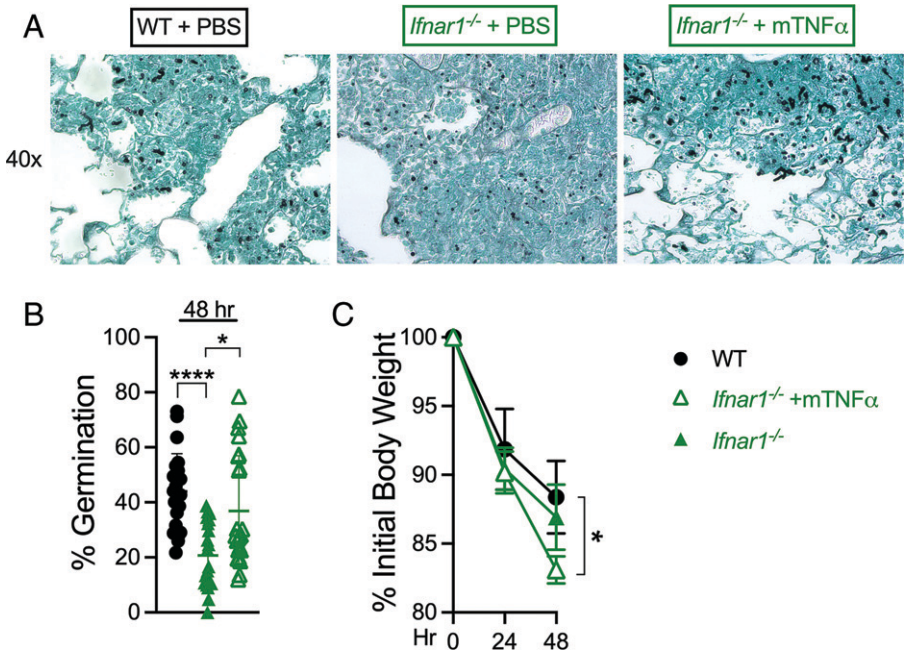

FIGURE 7. Role for TNF-α in damage and fungal clearance during *A. fumigatus* infection in WT and *Ifnar1*$^{-/-}$ mice. WT and *Ifnar1*$^{-/-}$ mice were infected with 8×10^7 *A. fumigatus* conidia i.t. on day 0 and were treated with mTNF-α or PBS i.n. at 6 and 30 h p.i. (**A**) Representative images from GMS (×40)-stained lung sections from 48 h p.i., (**B**) percent germination at 48 h p.i. (data are shown as the combined results from multiple images), and (**C**) weight loss as a percent of day 0 (initial body weight) were measured. Two independent experiments were performed, and data are shown as the combined results (WT group, $n = 8$; *Ifnar1*$^{-/-}$ + mTNF-α group, $n = 8$; *Ifnar1*$^{-/-}$ group, $n = 6$). The Kruskal-Wallis test with Dunn's multiple comparisons was performed for statistical analyses. All error bars represent SDs. $^*p < 0.05$, $^{****}p < 0.0001$.

TNF-α is sufficient to alter the *Ifnar1*$^{-/-}$ mice fungal clearance and damage phenotype, other damaging/inflammatory mediators are likely required because we did not find a full restoration of the *Ifnar2*$^{-/-}$ phenotype.

Discussion

Long-term immune suppression is known to be a factor predisposing patients to acquiring fungal infections (2, 6, 43). However, there is an increasing incidence of transiently immunosuppressed or injured lung conditions that similarly are creating fungal permissive environments (6). Specifically, the increasing number of reports highlighting the growing threat and occurrence of secondary fungal infections in patients with severe respiratory viral infections (10–14, 31–33), including influenza and SARS-CoV-2, suggest that antiviral host responses could create such an environment. As far as the antiviral mechanism involved in generating this transient immune suppression allowing for secondary infections to occur, type I IFN signaling has been identified by multiple groups, including ours (15–19). Our recent evidence suggested that type I IFN signaling is controlling the immune status of the lung through regulation of damage responses (20). Because host tissue damage is one of the main factors involved in the pathological outcome to IPA in humans, we sought to investigate the involvement of IFNAR signaling in *A. fumigatus* infection outcome and severity.

Increasing evidence suggests the existence of distinct type I IFN signaling via IFNAR1 or IFNAR2, and that these individual receptors have separate functions in relation to disease outcomes. In early studies on type I IFNs, it was found that Ab neutralization of only IFNAR1 blocked the activity of IFNα, but not IFN-β (44). Further, expanding on these studies, there is increasing evidence of IFNAR2 being able to signal as a homodimer (44–46). Specifically, these studies show that when the transmembrane and intracellular portion of IFNAR2 are attached to a different extracellular domain (EPO, IFN-γ R2/R1, nanobodies) upon their ligand addition/binding, the two IFNAR2 subunits dimerize and downstream ISGs are induced. These studies suggest the possibility of the existence of IFNAR2 homodimer signaling contributing to the IFN responses. Recent evidence also suggests that in the case of human IFNAR signaling that there may be more than one binding site on IFNAR2's intracellular domain for STAT2, suggesting that these binding sites may play a role in the downstream signals in terms of the genes induced and the level of that induction (47). In the case of murine IFNAR signaling, it was also previously demonstrated that there is differential gene expression after stimulation of *Ifnar1*$^{-/-}$ and *Ifnar2*$^{-/-}$ peritoneal exudate cells with IFN-β (48). Specifically, when *Ifnar2*$^{-/-}$ peritoneal exudate cells were stimulated with IFN-β, they did not induce conventional Jak/STAT signaling but induced >100 unique genes compared with WT cells.

Further supporting the independent function of these IFNAR subunits, we previously demonstrated that treatment with rIFN-β at the time of infection rescued *Ifnar1*$^{-/-}$ mice, but not *Ifnar2*$^{-/-}$ mice, from lethal IAV infection (20). Neutralizing IFN-β during IAV infection in WT mice resulted in increased susceptibility to secondary bacterial infection, suggesting the protective role for IFN-β signaling for secondary infection outcome (15). Importantly, similar treatment with rIFN-αA at the time of infection did not rescue the WT, *Ifnar2*$^{-/-}$, or *Ifnar1*$^{-/-}$ mice from lethal influenza infection (20). These results support a mechanism involving IFN-β–IFNAR2 signaling in protection from IAV infection. We also determined that the individual IFNAR subunits differentially regulate the morbidity and mortality to IAV, with IFNAR2 being associated with damage regulation (20). Importantly, multiple reports from the COVID-19 pandemic examining genetic factors involved in susceptibility and disease severity have identified loss of function and/or decreased levels of IFNAR2 as a COVID-19 severity risk factor (49–56). In addition, a decreased type I IFN response has also been associated with COVID-19 disease severity (57–60), further suggesting that type I IFN responses are important in regulating the lung environment during infection. Combined with the increasing prevalence of secondary fungal infections in patients with COVID-19, this suggested that virus-induced alterations in type I IFN signaling may be involved in control of fungal susceptibility.

Although previous work established a role for IFNAR1 in being critical for clearance from *A. fumigatus* infection (24), our study revealed a role for IFNAR2 in regulating damage during infection. We found that the IFNAR2 subunit is required for effective regulation of the damage response that occurs during *A. fumigatus* pulmonary infection. Moreover, our results suggest that IFNAR2 may interfere with IFNAR1-medaited fungal clearance, because *Ifnar2*$^{-/-}$ mice were more efficient at clearing conidia compared with WT mice. Thus, our results indicate that IFNAR1 is important for fungal clearance, whereas IFNAR2 is important for regulating inflammation and the associated damage/injury. Thus, it is tempting to speculate that the lung environment of *Ifnar2*$^{-/-}$ mice may be similar to what is found in the early stages of acute lung injury (ALI), where disruption of the alveolar–capillary barrier is followed by pulmonary inflammation via activation of APCs in the lungs, subsequent production of cytokines and chemokines, and recruitment of leukocytes (61).

Importantly, although we found early clearance of conidia in the *Ifnar2*$^{-/-}$ mice, our data suggest that the damaged/inflamed lung environment in the *Ifnar2*$^{-/-}$ mice creates an optimal niche for invasive growth of *A. fumigatus* to occur. Because we did not find elevated levels of TNF-α during IAV infection in the *Ifnar2*$^{-/-}$ mice (20), this suggests that the TNF-α damage response in the *Ifnar2*$^{-/-}$ mice is being driven by *A. fumigatus*, specifically in the absence of IFNAR2. Likely, the increased inflammatory response during the early stage of *A. fumigatus* infection (<24 h) is aiding in the increased conidial clearance, but without regulation of the damage and inflammation (>24 h) this environment becomes detrimental to the infection outcome by favoring fungal growth. This is supported by our results demonstrating that neutralization of TNF-α in the *Ifnar2*$^{-/-}$ mice leads not only to decreased conidial clearance but also to a modest decrease in damage. In patients, elevated levels of TNF-α are associated with ALI, and even more so with progressive acute respiratory distress syndrome (37, 62). In addition, progressive lung injury is one of the hallmarks of *Aspergillus* infection in patients with chronic granulomatous disease (CGD), which is characterized by a hyperinflammatory/damage response (63). Consistent with the detrimental role of hyperinflammation in CGD, neutralization of TNF-α in a CGD mouse model prevented lung injury during *Aspergillus* infection (64), supporting a role for TNF-α in creating a damaged lung environment. However, TNF-α is likely not the only important factor in inflamed lung environments because there was a lack of observed benefits from multiple clinical trials and studies aiming to block TNF-α responses in ALI and acute respiratory distress syndrome (65–67), alluding to this damage/injury mechanism being far more complicated. TNF-α is also known to be one of the mechanisms involved in activating type I IFNs, specifically IFN-β (68), and can induce sustained IFN responses through an IFN-mediated autocrine loop. Because we did not find a significant decrease in neutrophil recruitment in the *Ifnar2*$^{-/-}$ mice after TNF-α blocking (as has been found to occur in WT mice [42]), this further suggests existence of a TNF-IFN mechanism that is involved in the damage response. This may involve known TNF-effector cell responses, such as regulation of reactive oxygen species or cell death pathways (69). It was recently demonstrated that

TNF-α and IFN-γ are both required to induce inflammatory cell death via PANoptosis (P, pyroptosis; A, apoptosis; N, necroptosis) during SARS-CoV-2 infection, and that this mechanism contributes to the inflammatory-mediated mortality associated with SARS-CoV-2 infection (70). Although this mechanism may be specific to viral or SARS-CoV-2 infections, there is also the possibility it is involved in the IFNAR2 damage response during *A. fumigatus* infection because there is a strong indication for type I IFN signaling in viral infection pathology (14, 20, 71, 72). Based on our results, it will be important to determine whether TNF-α activation of the downstream signaling pathways leads to induction of IFN-β and whether IFN-β–IFNAR1 signaling in the *Ifnar2*$^{-/-}$ mice plays a role in creating the damaging environment as infection progresses. In addition, there may also be a role for IL-1 signaling in damage responses because previous data demonstrated that neutralizing IL-1R signaling in the CGD mouse model decreased inflammation and restored host control of *A. fumigatus*. Because we found that IL-1α was increased in the *Ifnar2*$^{-/-}$ mice compared with *Ifnar1*$^{-/-}$ mice, this may suggest that IL-1 signaling could also be contributing to the damage response in the *Ifnar2*$^{-/-}$ mice.

The specific pattern recognition receptors, whether extracellular or intracellular (73), that are involved in this TNF-IFNAR signaling mechanism controlling lung damage during infection remain unknown. It is well established that TNF-α production is a major outcome from engagement of Dectin-1 with surface-exposed β-glucan (74–77). In addition, it was also recently shown that Dectin-1 recognition of β-glucan from *A. fumigatus* was required for the initiation of type I and type III IFN expression, and that the antifungal response of *Dectin-1*$^{-/-}$ mice could be rescued by treatment with recombinant mouse type I and III IFNs (34). Although these results suggest that Dectin-1 is involved in TNF-α activation and the response to *A. fumigatus* infection, it will be important to determine whether these same mechanisms are involved both during and after the antiviral response. The antiviral host responses induced during viral infection may have a role in shaping the host responses to fungal challenge, including recognition and activation of TNF-α, that are separate from those found to occur during primary fungal infection.

Because fungal-associated PAMPs are not accessible to pattern recognition receptors on *A. fumigatus* conidia, it is well accepted that morphological change to swollen conidia (germination) proceeds recognition of *A. fumigatus* by innate immune cells. However, our results suggest that in the absence of IFNAR2, both inflammatory and damage responses are induced in the lung by *A. fumigatus* conidia. This may likely be because of activation of type I IFNs by the lung epithelial cells, because previous work has demonstrated that respiratory epithelial cells recognize resting conidia and induce IFN-β– and IFN-inducible genes (78). In addition, induction of IFN-α was reported to occur as early as 3 h after *A. fumigatus* infection, further suggesting that there may be a role for epithelial induction of type I IFNs. However, alveolar macrophages have also been shown to produce IFN-β after viral infection, and this IFN-β production was involved in inducing ALI (72). It was also recently demonstrated that alveolar macrophage induction of mitochondrial antiviral-signaling protein-dependent IFN responses was required to maintain host resistance to *A. fumigatus* infection (38). These studies support a role for antiviral IFN signaling responses in alveolar macrophages in both lung damage and fungal resistance. Based on our results, because we saw markers of damage early during *A. fumigatus* infection (6 h) in the *Ifnar2*$^{-/-}$ mice, this suggests that IFNAR2 signaling from the epithelium, alveolar macrophages, or a combination of both may be required to regulate damage/injury in the lung early during infection.

Our study revealed that IFNAR2 is required for effective regulation of the damage response that occurs during *A. fumigatus* pulmonary infection. Importantly, our study supports the likely role for aberrant type I IFN signaling in contributing to an *A. fumigatus*–permissive environment through regulation of inflammation. Moreover, our results also further support the concept of unique contributions from both IFNAR1 and IFNAR2 that had been established by both our group (15, 20) and others (47, 48, 79–81). Because we previously found evidence of increased tissue damage after IAV infection in the *Ifnar2*$^{-/-}$ mice (20), combined with our data presented in this article, this suggests that IFNAR2 regulation of the damage response may be a more general host mechanism induced in response to infection in the lung. However, the downstream mediators involved in the damage response are likely more complex because we did not find significant differences in TNF-α during IAV infection (20), further highlighting the need for determining these mechanisms. Although we have not excluded the importance of the other damage biomarkers we observed, our data reveal that neutralization of TNF-α can help to mitigate at least some of the damage and morbidity phenotypes of the *Ifnar2*$^{-/-}$ mice during *A. fumigatus* infection. Moving forward, it will be essential to determine the mechanisms involved in IFNAR regulation of damage and antifungal immunity, both upstream and downstream, to potentially better inform design of treatments aimed at minimizing damage in patients with IPA or controlling pulmonary tissue damage.

Acknowledgments

We thank Amariliz Rivera for valuable discussion and Joshua J. Obar for valuable discussion, comments, and suggestions. We acknowledge the Stem Cell Instrumentation Foundry for assistance in generating flow cytometry data.

Disclosures

The authors have no financial conflicts of interest.

References

1. Bongomin, F. S. Gago, R. O. Oladele, and D. W. Denning. 2017. Global and multi-national prevalence of fungal diseases—estimate precision. *J. Fungi* 3: 57.
2. Baddley, J. W., D. R. Andes, K. A. Marr, D. P. Kontoyiannis, B. D. Alexander, C. A. Kauffman, R. A. Oster, E. J. Anaissie, T. J. Walsh, M. G. Schuster, et al. 2010. Factors associated with mortality in transplant patients with invasive aspergillosis. *Clin. Infect. Dis.* 50: 1559–1567.
3. Aguilar, C. A., B. Hamandi, C. Fegbeutel, F. P. Silveira, E. A. Verschuuren, P. Ussetti, P. V. Chin-Hong, A. Sole, C. Holmes-Liew, E. M. Billaud, et al. 2018. Clinical risk factors for invasive aspergillosis in lung transplant recipients: results of an international cohort study. *J. Heart Lung Transplant.* 37: 1226–1234.
4. Upton, A., K. A. Kirby, P. Carpenter, M. Boeckh, and K. A. Marr. 2007. Invasive aspergillosis following hematopoietic cell transplantation: outcomes and prognostic factors associated with mortality. *Clin. Infect. Dis.* 44: 531–540.
5. Szalewski, D. A., V. S. Hinrichs, D. K. Zinniel, and R. G. Barletta. 2018. The pathogenicity of *Aspergillus fumigatus*, drug resistance, and nanoparticle delivery. *Can. J. Microbiol.* 64: 439–453.
6. Kousha, M. R. Tadi, and A. O. Soubani. 2011. Pulmonary aspergillosis: a clinical review. *Eur. Respir. Rev.* 20: 156–174.
7. Carvalho, A., C. Cunha, R. G. Iannitti, A. D. Luca, G. Giovannini, F. Bistoni, and L. Romani. 2012. Inflammation in aspergillosis: the good, the bad, and the therapeutic. *Ann. N Y Acad. Sci.* 1273: 52–59.
8. Ader, F., A.-L. Bienvenu, B. Rammaert, and S. Nseir. 2009. Management of invasive aspergillosis in patients with COPD: rational use of voriconazole. *Int. J. Chron. Obstruct. Pulmon. Dis.* 4: 279–287.
9. Uzunhan, Y., H. Nunes, F. Jeny, M. Lacroix, S. Brun, P.-Y. Brillet, E. Martinod, M.-F. Carette, D. Bouvry, C. Charlier, et al. 2017. Chronic pulmonary aspergillosis complicating sarcoidosis. *Eur. Respir. J.* 49: 1602396.
10. Vanderbeke, L. I. Spriet, C. Breynaert, B. J. A. Rijnders, P. E. Verweij, and J. Wauters. 2018. Invasive pulmonary aspergillosis complicating severe influenza: epidemiology, diagnosis and treatment. *Curr. Opin. Infect. Dis.* 31: 471–480.
11. Shah, M. M., E. I. Hsiao, C. M. Kirsch, A. Gohil, S. Narasimhan, and D. A. Stevens. 2018. Invasive pulmonary aspergillosis and influenza co-infection in immunocompetent hosts: case reports and review of the literature. *Diagn. Microbiol. Infect. Dis.* 91: 147–152.
12. Talento, A. F., K. Dunne, N. Murphy, B. O'Connell, G. Chan, E. A. Joyce, F. Hagen, J. F. Meis, R. Fahy, L. Bacon, et al. 2018. Post-influenzal triazole-resistant aspergillosis following allogeneic stem cell transplantation. *Mycoses* 61: 570–575.

13. Rouzé, A., E. Lemaitre, I. Martin-Loeches, P. Povoa, E. Diaz, R. Nyga, A. Torres, M. Metzelard, D. D. Cheyron, F. Lambiotte, et al.; coVAPid study group. 2022. Invasive pulmonary aspergillosis among intubated patients with SARS-CoV-2 or influenza pneumonia: a European multicenter comparative cohort study. *Crit. Care* 26: 11.
14. Beumer, M. C., R. M. Koch, D. van Beuningen, A. M. OudeLashof, F. L. van de Veerdonk, E. Kolwijck, J. G. van der Hoeven, D. C. Bergmans, and C. W. E. Hoedemaekers. 2019. Influenza virus and factors that are associated with ICU admission, pulmonary co-infections and ICU mortality. *J. Crit. Care* 50: 59–65.
15. Shepardson, K. M., K. Larson, R. V. Morton, J. R. Prigge, E. E. Schmidt, V. C. Huber, and A. Rynda-Apple. 2016. Differential type I interferon signaling is a master regulator of susceptibility to postinfluenza bacterial superinfection. *Mbio* 7: e00506-16.
16. Shahangian, A., E. K. Chow, X. Tian, J. R. Kang, A. Ghaffari, S. Y. Liu, J. A. Belperio, G. Cheng, and J. C. Deng. 2009. Type I IFNs mediate development of postinfluenza bacterial pneumonia in mice. *J. Clin. Invest.* 119: 1910–1920.
17. Lee, B., K. M. Robinson, K. J. McHugh, E. V. Scheller, S. Mandalapu, C. Chen, Y. P. Di, M. E. Clay, R. I. Enelow, P. J. Dubin, and J. F. Alcorn. 2015. Influenza-induced type I interferon enhances susceptibility to gram-negative and gram-positive bacterial pneumonia in mice. *Am. J. Physiol. Lung Cell. Mol. Physiol.* 309: L158–L167.
18. Sun, K., and D. W. Metzger. 2008. Inhibition of pulmonary antibacterial defense by interferon-γ during recovery from influenza infection. *Nat. Med.* 14: 558–564.
19. Metzger, D. W., and K. Sun. 2013. Immune dysfunction and bacterial coinfections following influenza. *J. Immunol.* 191: 2047–2052.
20. Shepardson, K. M., K. Larson, L. L. Johns, K. Stanek, H. Cho, J. Wellham, H. Henderson, and A. Rynda-Apple. 2018. IFNAR2 is required for anti-influenza immunity and alters susceptibility to post-influenza bacterial superinfections. *Front. Immunol.* 9: 2589.
21. Prigge, J. R., T. R. Hoyt, E. Dobrinen, M. R. Capecchi, E. E. Schmidt, and N. Meissner. 2015. Type I IFNs act upon hematopoietic progenitors to protect and maintain hematopoiesis during pneumocystis lung infection in mice. *J. Immunol.* 195: 5347–5357.
22. Hubrecht, R. 2011. *Guide for the Care and Use of Laboratory Animals, Eighth Edition 2011.* The Committee for the Update of the Guide for the Care and Use of Laboratory Animals (2011). Published by the National Research Council of the National Academies, Washington DC, USA. 219 pp Paperback (ISBN 0-309-15400-6). Price US$19.95. *Anim. Welf.* 20: 455–456.
23. Shepardson, K. M., A. Jhingran, A. Caffrey, J. J. Obar, B. T. Suratt, B. L. Berwin, T. M. Hohl, and R. A. Cramer. 2014. Myeloid derived hypoxia inducible factor 1-alpha is required for protection against pulmonary *Aspergillus fumigatus* infection. *PLoS Pathog.* 10: e1004378.
24. Espinosa, V., O. Dutta, C. McElrath, P. Du, Y.-J. Chang, B. Cicciarelli, A. Pitler, I. Whitehead, J. J. Obar, J. E. Durbin, et al. 2017. Type III interferon is a critical regulator of innate antifungal immunity. *Sci. Immunol.* 2: eaan5357.
25. Li, H., B. M. Barker, N. Grahl, S. Puttikamonkul, J. D. Bell, K. D. Craven, and R. A. Cramer. 2011. The small GTPase RacA mediates intracellular reactive oxygen species production, polarized growth, and virulence in the human fungal pathogen Aspergillus fumigatus. *Eukaryot. Cell.* 10: 174–186.
26. Caffrey-Carr, A. K., C. H. Kowalski, S. R. Beattie, N. A. Blaseg, C. R. Upshaw, A. Thammahong, H. E. Lust, Y.-W. Tang, T. M. Hohl, R. A. Cramer, and J. J. Obar. 2017. Interleukin 1α is critical for resistance against highly virulent *Aspergillus fumigatus* isolates. *Infect. Immun.* 85: e00661-17.
27. Liu, K.-W., M. S. Grau, J. T. Jones, X. Wang, E. M. Vesely, M. R. James, C. Gutierrez-Perez, R. A. Cramer, and J. J. Obar. 2022. Postinfluenza environment reduces *Aspergillus fumigatus* conidium clearance and facilitates invasive aspergillosis *in vivo*. *Mbio* 13: e0285422.
28. van de Veerdonk, F. L., E. Kolwijck, P. P. A. Lestrade, C. J. Hodiamont, B. J. A. Rijnders, J. van Paassen, P.-J. Haas, C. O. dos Santos, G. A. Kampinga, et al.; Dutch Mycoses Study Group. 2017. Influenza-associated Aspergillosis in critically ill patients. *Am. J. Respir. Crit. Care Med.* 196: 524–527.
29. Lat, A., N. Bhadelia, B. Miko, E. Y. Furuya, and G. R. Thompson. 2010. Invasive Aspergillosis after pandemic (H1N1) 2009. *Emerg. Infect. Dis.* 16: 971–973.
30. Wauters, J., I. Baar, P. Meersseman, W. Meersseman, K. Dams, R. D. Paep, K. Lagrou, A. Wilmer, P. Jorens, and G. Hermans. 2012. Invasive pulmonary aspergillosis is a frequent complication of critically ill H1N1 patients: a retrospective study. *Intensive Care Med.* 38: 1761–1768.
31. Kwon, O. K., M. G. Lee, H. S. Kim, M. S. Park, K. M. Kwak, and S. Y. Park. 2013. Invasive pulmonary aspergillosis after influenza A infection in an immunocompetent patient. *Tuberc. Respir. Dis. (Seoul)*. 75: 260–263.
32. Crum-Cianflone, N. F. 2016. Invasive aspergillosis associated with severe influenza infections. *Open Forum Infect. Dis.* 3: ofw171.
33. Nulens, E. F., M. J. Bourgeois, and M. B. Reynders. 2017. Post-influenza aspergillosis, do not underestimate influenza B. *Infect. Drug Resist.* 10: 61–67.
34. Dutta, O., V. Espinosa, K. Wang, S. Avina, and A. Rivera. 2020. Dectin-1 promotes type I and III interferon expression to support optimal antifungal immunity in the lung. *Front. Cell. Infect. Microbiol.* 10: 321.
35. Guo, Y., S. Kasahara, A. Jhingran, N. L. Tosini, B. Zhai, M. A. Aufiero, K. A. M. Mills, M. Gjonbalaj, V. Espinosa, A. Rivera, et al. 2020. During aspergillus infection, monocyte-derived DCs, neutrophils, and plasmacytoid DCs enhance innate immune defense through CXCR3-dependent crosstalk. *Cell Host Microbe* 28: 104–116.e4.
36. Su, X., M. R. Looney, N. Gupta, and M. A. Matthay. 2009. Receptor for advanced glycation end-products (RAGE) is an indicator of direct lung injury in models of experimental lung injury. *Am. J. Physiol. Lung Cell. Mol. Physiol.* 297: L1–L5.
37. Wada, T., S. Jesmin, S. Gando, Y. Yanagida, A. Mizugaki, S. N. Sultana, S. Zaedi, and H. Yokota. 2013. The role of angiogenic factors and their soluble receptors in acute lung injury (ALI)/acute respiratory distress syndrome (ARDS) associated with critical illness. *J. Inflamm. (Lond).* 10: 6.
38. Wang, X., C. Cunha, M. S. Grau, S. J. Robertson, J. F. Lacerda, A. Campos, K. Lagrou, J. Maertens, S. M. Best, A. Carvalho, and J. J. Obar. 2022. MAVS expression in alveolar macrophages is essential for host resistance against *Aspergillus fumigatus*. *J. Immunol.* 209: 346–353.
39. Caffrey, A. K., M. M. Lehmann, J. M. Zickovich, V. Espinosa, K. M. Shepardson, C. P. Watschke, K. M. Hilmer, A. Thammahong, B. M. Barker, A. Rivera, et al. 2015. IL-1α signaling is critical for leukocyte recruitment after pulmonary *Aspergillus fumigatus* challenge. *PLoS Pathog.* 11: e1004625.
40. Caffrey-Carr, A. K., K. M. Hilmer, C. H. Kowalski, K. M. Shepardson, R. M. Temple, R. A. Cramer, and J. J. Obar. 2018. Host-derived leukotriene B4 is critical for resistance against invasive pulmonary aspergillosis. *Front. Immunol.* 8: 1984.
41. Rodrigues, A. G., R. Araujo, and C. Pina-Vaz. 2005. Human albumin promotes germination, hyphal growth and antifungal resistance by *Aspergillus fumigatus*. *Med. Mycol.* 43: 711–717.
42. Mehrad, B., R. M. Strieter, and T. J. Standiford. 1999. Role of TNF-α in pulmonary host defense in murine invasive aspergillosis. *J. Immunol.* 162: 1633–1640.
43. Russo, A., G. Tiseo, M. Falcone, and F. Menichetti. 2020. Pulmonary aspergillosis: an evolving challenge for diagnosis and treatment. *Infect. Dis. Ther.* 9: 511–524.
44. Pattyn, E., X. V. Ostade, L. Schauvliege, A. Verhee, M. Kalai, J. Vandekerckhove, and J. Tavernier. 1999. Dimerization of the interferon type I receptor IFNaR2–2 is sufficient for induction of interferon effector genes but not for full antiviral activity. *J. Biol. Chem.* 274: 34838–34845.
45. Zoellner, N., N. Coesfeld, F. H. D. Vos, J. Denter, H. C. Xu, E. Zimmer, B. Knebel, H. Al-Hasani, S. Mossner, P. A. Lang, et al. 2022. Synthetic mimetics assigned a major role to IFNAR2 in type I interferon signaling. *Front. Microbiol.* 13: 947169.
46. Kotenko, S. V., L. S. Izotova, O. V. Mirochnitchenko, C. Lee, and S. Pestka. 1999. The intracellular domain of interferon-α receptor 2c (IFN-αR2c) chain is responsible for Stat activation. *Proc. Natl Acad. Sci. USA* 96: 5007–5012.
47. Shemesh, M., S. Lochte, J. Piehler, and G. Schreiber. 2021. IFNAR1 and IFNAR2 play distinct roles in initiating type I interferon–induced JAK-STAT signaling and activating STATs. *Sci. Signal.* 14: eabe4627.
48. de Weerd, N. A., J. P. Vivian, T. K. Nguyen, N. E. Mangan, J. A. Gould, S.-J. Braniff, L. Zaker-Tabrizi, K. Y. Fung, S. C. Forster, T. Beddoe, et al. 2013. Structural basis of a unique interferon-β signaling axis mediated via the receptor IFNAR1. *Nat. Immunol.* 14: 901–907.
49. Pairo-Castineira, E., S. Clohisey, L. Klaric, A. D. Bretherick, K. Rawlik, D. Pasko, S. Walker, N. Parkinson, M. H. Fourman, C. D. Russell, et al. 2021. Genetic mechanisms of critical illness in COVID-19. *Nature* 591: 92–98.
50. Velavan, T. P., S. R. Pallerla, J. Rüter, Y. Augustin, P. G. Kremsner, S. Krishna, and C. G. Meyer. 2021. Host genetic factors determining COVID-19 susceptibility and severity. *EbioMedicine* 72: 103629.
51. Baranova, A., H. Cao, and F. Zhang. 2021. Unraveling risk genes of COVID-19 by multi-omics integrative analyses. *Front. Med. (Lausanne)* 8: 738687.
52. Ma, Y., Y. Huang, S. Zhao, Y. Yao, Y. Zhang, J. Qu, N. Wu, and J. Su. 2021. Integrative genomics analysis reveals a 21q22.11 locus contributing risk to COVID-19. *Hum. Mol. Genet.* 30: 1247–1258.
53. Gaziano, L., C. Giambartolomei, A. C. Pereira, A. Gaulton, D. C. Posner, S. A. Swanson, Y.-L. Ho, S. K. Iyengar, N. M. Kosik, M. Vujkovic, et al.; VA Million Veteran Program COVID-19 Science Initiative. 2021. Actionable druggable genome-wide Mendelian randomization identifies repurposing opportunities for COVID-19. *Nat. Med.* 27: 668–676.
54. Smieszek, S. P., V. M. Polymeropoulos, C. Xiao, C. M. Polymeropoulos, and M. H. Polymeropoulos. 2021. Loss of function mutations in the IFNAR2 in COVID-19 severe infection susceptibility. *J. Glob. Antimicrob. Resist.* 26: 239–240.
55. Liu, D., J. Yang, B. Feng, W. Lu, C. Zhao, and L. Li. 2021. Mendelian randomization analysis identified genes pleiotropically associated with the risk and prognosis of COVID-19. *J. Infect.* 82: 126–132.
56. Akter, S., A. S. Roy, M. I. Q. Tonmoy, and M. S. Islam. 2022. Deleterious single nucleotide polymorphisms (SNPs) of human IFNAR2 gene facilitate COVID-19 severity in patients: a comprehensive in silico approach. *J. Biomol. Struct. Dyn.* 40: 11173–11189.
57. Zhou, W., and W. Wang. 2021. Auto-antibodies against type I IFNs are associated with severe COVID-19 pneumonia. *Signal Transduct. Target. Ther.* 6: 96.
58. Goncalves, D., M. Mezidi, P. Bastard, M. Perret, K. Saker, N. Fabien, R. Pescarmona, C. Lombard, T. Walzer, J. Casanova, et al. 2021. Antibodies against type I interferon: detection and association with severe clinical outcome in COVID-19 patients. *Clin. Transl. Immunol.* 10: e1327.
59. Hadjadj, J., N. Yatim, L. Barnabei, A. Corneau, J. Boussier, N. Smith, H. Péré, B. Charbit, V. Bondet, C. Chenevier-Gobeaux, et al. 2020. Impaired type I interferon activity and inflammatory responses in severe COVID-19 patients. *Science* 369: 718–724.
60. Troya, J., P. Bastard, L. Planas-Serra, P. Ryan, M. Ruiz, M. de Carranza, J. Torres, A. Martínez, L. Abel, J.-L. Casanova, and A. Pujol. 2021. Neutralizing autoantibodies to type I IFNs in >10% of patients with severe COVID-19 pneumonia hospitalized in Madrid, Spain. *J. Clin. Immunol.* 41: 914–922.
61. Johnson, E. R., and M. A. Matthay. 2010. Acute lung injury: epidemiology, pathogenesis, and treatment. *J. Aerosol Med. Pulm. Drug Deliv.* 23: 243–252.
62. Patel, B. V., M. R. Wilson, K. P. O'Dea, and M. Takata. 2013. TNF-induced death signaling triggers alveolar epithelial dysfunction in acute lung injury. *J. Immunol.* 190: 4274–4282.
63. Segal, B. H., P. Veys, H. Malech, and M. J. Cowan. 2011. Chronic granulomatous disease: lessons from a rare disorder. *Biol. Blood Marrow Transplant.* 17: S123–S131.

64. Cagnina, R. E., K. R. Michels, A. M. Bettina, M. D. Burdick, Y. Scindia, Z. Zhang, T. J. Braciale, and B. Mehrad. 2021. Neutrophil-derived tumor necrosis factor drives fungal acute lung injury in chronic granulomatous disease. *J. Infect. Dis.* 224: 1225–1235.
65. Fisher, C. J., J. M. Agosti, S. M. Opal, S. F. Lowry, R. A. Balk, J. C. Sadoff, E. Abraham, R. M. H. Schein, and E. Benjamin. 1996. Treatment of septic shock with the tumor necrosis factor receptor:Fc fusion protein. *N Engl. J. Med.* 334: 1697–1702.
66. Proudfoot, A., A. Bayliffe, C. M. O'Kane, T. Wright, A. Serone, P. J. Bareille, V. Brown, U. I. Hamid, Y. Chen, R. Wilson, et al. 2018. Novel anti-tumour necrosis factor receptor-1 (TNFR1) domain antibody prevents pulmonary inflammation in experimental acute lung injury. *Thorax* 73: 723–730.
67. Abraham, E., A. Anzueto, G. Gutierrez, S. Tessler, G. S. Pedro, R. Wunderink, A. D. Nogare, S. Nasraway, S. Berman, R. Cooney, et al.; NORASEPT II Study Group. 1998. Double-blind randomised controlled trial of monoclonal antibody to human tumour necrosis factor in treatment of septic shock. *Lancet* 351: 929–933.
68. Mukhopadhyay, S., J. R. Hoidal, and T. K. Mukherjee. 2006. Role of TNFα in pulmonary pathophysiology. *Respir. Res.* 7: 125.
69. Blaser, H., C. Dostert, T. W. Mak, and D. Brenner. 2016. TNF and ROS crosstalk in inflammation. *Trends Cell Biol.* 26: 249–261.
70. Karki, R., B. R. Sharma, S. Tuladhar, E. P. Williams, L. Zalduondo, P. Samir, M. Zheng, B. Sundaram, B. Banoth, R. K. S. Malireddi, et al. 2021. Synergism of TNF-α and IFN-γ triggers inflammatory cell death, tissue damage, and mortality in SARS-CoV-2 infection and cytokine shock syndromes. *Cell* 184: 149–168.e17.
71. García-Sastre, A., R. K. Durbin, H. Zheng, P. Palese, R. Gertner, D. E. Levy, and J. E. Durbin. 1998. The role of interferon in influenza virus tissue tropism. *J. Virol.* 72: 8550–8558.
72. Högner, K., T. Wolff, S. Pleschka, S. Plog, A. D. Gruber, U. Kalinke, H.-D. Walmrath, J. Bodner, S. Gattenlöhner, P. Lewe-Schlosser, et al. 2013. Macrophage-expressed IFN-β contributes to apoptotic alveolar epithelial cell injury in severe influenza virus pneumonia. *PLoS Pathog.* 9: e1003188.
73. Wang, X., A. K. Caffrey-Carr, K. Liu, V. Espinosa, W. Croteau, S. Dhingra, A. Rivera, R. A. Cramer, and J. J. Obar. 2020. MDA5 is an essential sensor of a pathogen-associated molecular pattern associated with vitality that is necessary for host resistance against *Aspergillus fumigatus*. *J. Immunol.* 205: 3058–3070.
74. Taylor, P. R., S. V. Tsoni, J. A. Willment, K. M. Dennehy, M. Rosas, H. Findon, K. Haynes, C. Steele, M. Botto, S. Gordon, and G. D. Brown. 2007. Dectin-1 is required for β-glucan recognition and control of fungal infection. *Nat. Immunol.* 8: 31–38.
75. Werner, J. L., A. E. Metz, D. Horn, T. R. Schoeb, M. M. Hewitt, L. M. Schwiebert, I. Faro-Trindade, G. D. Brown, and C. Steele. 2009. Requisite role for the dectin-1 β-glucan receptor in pulmonary defense against *Aspergillus fumigatus*. *J. Immunol.* 182: 4938–4946.
76. Hohl, T. M., H. L. V. Epps, A. Rivera, L. A. Morgan, P. L. Chen, M. Feldmesser, and E. G. Pamer. 2005. *Aspergillus fumigatus* triggers inflammatory responses by stage-specific β-glucan display. *PLoS Pathog.* 1: e30.
77. Brown, G. D., J. Herre, D. L. Williams, J. A. Willment, A. S. J. Marshall, and S. Gordon. 2003. Dectin-1 mediates the biological effects of β-glucans. *J. Exp. Med.* 197: 1119–1124.
78. Beisswenger, C., C. Hess, and R. Bals. 2012. *Aspergillus fumigatus* conidia induce interferon-signalling in respiratory epithelial cells. *Eur. Respir. J.* 39: 411–418.
79. de Weerd, N. A., A. Y. Matthews, P. R. Pattie, N. M. Bourke, S. S. Lim, J. P. Vivian, J. Rossjohn, and P. J. Hertzog. 2017. A hot spot on interferon α/β receptor subunit 1 (IFNAR1) underpins its interaction with interferon-β and dictates signaling. *J. Biol. Chem.* 292: 7554–7565.
80. Weerd, N. A., J. P. Vivian, S. S. Lim, S. U. Huang, and P. J. Hertzog. 2020. Structural integrity with functional plasticity: what type I IFN receptor polymorphisms reveal. *J. Leukoc. Biol.* 108: 909–924.
81. Sheehan, K. C. F., H. M. Lazear, M. S. Diamond, and R. D. Schreiber. 2015. Selective blockade of interferon-α and -β reveals their non-redundant functions in a mouse model of West Nile virus infection. *PLoS One.* 10: e0128636.